Winkelnkemper, T., F. Seitz: Simulation of historic and future atmospheric angular momentum effects on length-of-day variations with GCMs. In: Observing our Changing Earth, Sideris, M. (Ed.), IAG Symposia, Vol. 133, 447-454, Springer, Berlin, 2008.

DOI: 10.1007/978-3-540-85426-5_54

Simulation of past and future atmospheric effects on length-of-day variations with GCMs

Timo Winkelnkemper (1) and Florian Seitz (2)
(1) Meteorological Institute University of Bonn, Auf dem Hügel 20, 53121 Bonn, Germany
(2) Earth Oriented Space Science and Technology (ESPACE), Technische Universität München, Arcisstr. 21, 80290 Munich, Germany
e-mail: timo@uni-bonn.de, seitz@dgfi.badw.de

Abstract. This paper focuses on atmospherical effects on changes in length-of-day (ΔLOD). A 20_{th} century simulation has been carried using an ECHAM 5 standalone atmosphere general circulation model (GCM). The spectrum of the resulting time series for ΔLOD shows typical structure patterns which resemble geodetic observations.

Furthermore an atmospheric scenario run for the period between the year 2000 and 2100 driven by an A1B forcing scenario shows a strong increase in the axial atmospheric angular momentum (AAM) which implies a shortening of the length-of-day. For the scenario runs the coupled atmosphere ocean sea ice model ECHO-G has been used. The extent of the change in axial AAM exceeds results of former studies. For the year 2100 the model shows an increase in axial AAM of about 10 percent compared to present day conditions. The strongest trends in zonal windspeed are detected in the southern hemisphere for mid and higher latitudes in the upper troposphere.

Keywords. atmospheric angular momentum, AAM, Earth rotation, ERP, length-of-day, atmospheric excitation, climate change, ECHAM 5, ECHO-G

1 Introduction

General circulation models are able to simulate mass movements and mass concentrations on a global scale in a realistic way. Due to enormous mass displacements and relative movements (to the rotating Earth) the atmosphere and oceanic hydrosphere have an important impact on Earth rotation parameters (ERPs). On a subdaily to decadal scale the atmosphere and the oceanic hydrosphere explain nearly all variance of ERPs (Lambeck, 1980). Variations in ΔLOD are closely linked to variations in the axial AAM by conservation of total angular momentum. The conservation of total angular momentum of different subsystems can be expressed by the Liouville differential equation. The derivation of the relation between ΔLOD and axial AAM is straightforward from the Liouville differential equation (Munk and MacDonald, 1960), see Sect. 3.

In this paper we focus on the atmospheric effect on ΔLOD. Axial AAM changes are highly correlated with short-term changes in length-of-day. On interdiurnal to interannual time scales theses changes are the dominant excitation to variations in ΔLOD. On decadal time scales significant angular momentum transfer between the Earth's liquid core and solid mantle can be detected (Hide, 1969) and exceeds the axial AAM influence on ΔLOD.

Our research concentrates on the ability of the ECHAM 5 GCM to reproduce axial AAM variations associated with changes in ΔLOD. The simulation covers the period from 1880 to 2003. From the early 60ies space geodetic techniques allowed for the observation of the Earth's rotation with increasing accuracy. By now, a 45 year time series of ΔLOD is availble from the International Earth Rotation and Reference Systems Service (IERS).

Possible long term trends under a climate change scenario have been studied in previous investigations (de Viron, 2002; Rosen and Gutowski, 1992). As far as only atmospheric effects on ΔLOD are considered, those earlier studies predict an increase in global relative axial AAM for the 21_{st} century which is related with a slowing of the angular velocity of the Earth. The main reason for this was pointed out by Lorenz and de Weaver (2007) who detected significantly increased and stronger westerly winds in mid and high latitudes particularly in the southern hemisphere under a climate change scenario.

2 Atmospheric Simulations

For the atmospheric simulation from 1880 to 2003 runs with the GCM ECHAM 5.3.02 have been carried out (Roeckner et al., 2003). An ensemble of three runs has been created by disturbing the initial conditions. The latter were extracted from five year intervalls of a short preindustrial control run. To obtain realistic states of the atmosphere a broad set of forcing factors was used. It includes greenhouse gas concentrations, an aerosol climatology, volcanic aerosols, solar variability (Froehlich and Lean, 1998) and sea surface temperature (SST) data as well as sea ice concentration (SIC) data from the hadley centre's reconstruction. To avoid a systematic underestimation of variance when linearly interpolating from monthly means to daily values - as the model expects as input - a filter has been applied (Taylor et al., 1997) to the SST and SIC data. The resolution of the simulation is T63 in the horizontal and 31 layers in the vertical. This represents a global grid consisting of 192 times 96 gridpoints. The distance of two neighbouring grid points is 1.875°. This resolution allows to simulate small scale troughs which could have an impact on the globally integrated AAM.

The A1B scenario run for a time span of 200 years (2000 to 2200) was performed by the coupled atmosphere ocean sea ice model ECHO-G. It consists of the ECHAM 4 atmosphere GCM and the HOPE-G ocean model. These model runs were part of the 4th assesment report (AR) for the Intergovernmental Panel on Climate Change (IPCC). Figure 1 illustrates ECHO-G temperature anomaly projections for different scenarios. These projections show an increase of global temperature by nearly three degrees Kelvin for the A1B scenario compared to present day conditions. The resolution of these runs is T30 in the horizontal (corresponding to a grid spacing of 3.75°) and 19 layers in the vertical.

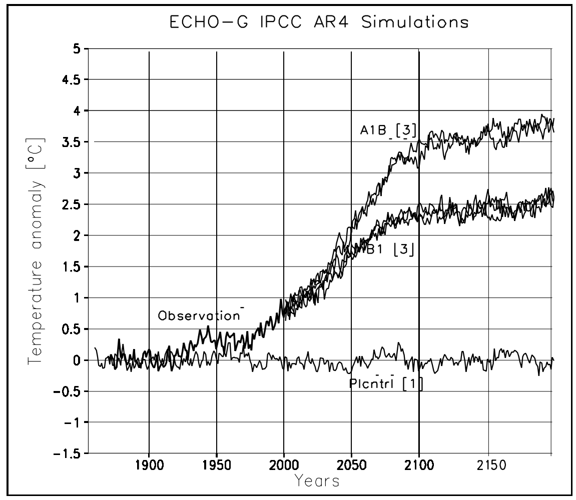

Figure 1: ECHO-G temperature anomalies for scenario A1B, B1 and PIcntrl (preindustrial control run)

3 Variations of △LOD

Angular momentum fluctuations in the various systems components of the Earth are related to temporal variations of Earth rotation. The solid Earth's reaction on the redistributions and motions of masses follows from the solution of the Liouville differential equation which describes the balance of angular momentum in a rotating reference frame:

$$\frac{d}{dt}\big(\underline{\mathbf{I}}\omega + \mathbf{h}\big) \; + \; \omega \times \big(\underline{\mathbf{I}}\omega + \mathbf{h}\big) \; = \; \mathbf{L}\,. \qquad (1)$$

In this equation $\mathbf{I}$ denotes the tensor of inertia of the Earth, $\mathbf{h}$ stands for angular momenta with respect to the reference frame (so-called relative angular momenta) and the vector $\mathbf{L}$ on the right hand side denotes torques which are mainly caused by the gravitational forces of Sun and Moon. The Earth rotation vector is denoted by ω. Due to the continuous redistribution and motion of mass elements in the Earth system, all quantities in Equation 1 are time-dependent.

Variations of Earth rotation are computed with respect to a uniformly rotating geocentric reference frame with its z-axis, about which it rotates, pointing approximately to the direction of the maximum moment of inertia. The angular velocity of the uniform rotation is one revolution per sidereal day: $\Omega = 2\pi/86164\mathrm{s}^{-1}$. Due to geophysical processes and gravitational torques this uniform rotation is slightly disturbed and the Earth rotation vector can be written as

$$\omega(t) \;=\; \Omega\cdot\begin{pmatrix} m_1(t) \\ m_2(t) \\ 1+m_3(t)\end{pmatrix}, \qquad m_i \ll 1\,. \quad (2)$$

The dimensionless quantities m_i denote small disturbances of the uniform rotation (Munk and McDonald, 1960). Fluctuations of the angular velocity of the Earth are equivalent to changes of length-of-day (ΔLOD). They follow from temporal variations of the absolute value of the Earth rotation vector $|\omega(t)|$, which are computed by

$$\begin{aligned} |\omega(t)| &= \Omega\sqrt{m_1(t)^2+m_2(t)^2+(1+m_3(t))^2} \\ &\approx \Omega(1+m_3(t)) \end{aligned} \quad (3)$$

The error of ΔLOD due to this approximation is in the order of 10^{-16} s and is negligible. The relation between the variations $|\omega(t)|$ and length-of-day changes follows from the definition of ΔLOD as the duration of one revolution of the Earth reduced by 86400 s:

$$\Delta\mathrm{LOD} = \frac{2\,\pi}{|\omega(t)|} - 86400\,\mathrm{s}\,. \quad (4)$$

When higher order terms and external torques are neglected, the insertion of Equation 2 into Equation 1 yields

$$m_3 = -[0.756\;\Omega\;\Delta I_{zz} + \Delta h_z]/\Omega C_m\;, \quad (5)$$

where the factor 0.756 accounts for the effect of load deformations of the solid Earth and C_m is the polar moment of inertia of the Earth's crust and mantle (Gross, 2004). Polar motion which is related to the temporal variation of $m_1(t)$ and $m_2(t)$ is not subject of this paper.

In the following we will focus on atmospheric effects on length-of-day changes. As mentioned it is well known that the largest part of observed variations of ΔLOD on time scales from months to a few years is caused by axial relative atmospheric angular momentum h_z^{AAM} due to zonal wind variations (Gross, 2004):

$$h_z^{AAM} = \int_{V_{atm}} \rho r^2(\mathbf{r}\times\mathbf{v})_z dV \quad (6)$$

$$h_z^{AAM} = \frac{r^3}{g}\int_\eta\int_\lambda\int_\varphi p_s u cos^2\varphi d\varphi d\lambda d\eta \quad (7)$$

Equation 7 shows the global mass integration over the atmosphere expressed in spherical coordinates. Zonal windspeed u and surface pressure p_s are obtained from the model's output. η is the standardized vertical coordinate of the atmospheric GCM. Boundaries of η are 0 for the top of the atmosphere and 1 for the Earth's surface.

4 Results

From the ECHAM 5 simulations a 2m-temperature anomaly time series has been derived. As the simulation is driven by observed or reconstructed SSTs and SICs, temperature measurements over the ocean were excluded because they are highly affected by the SST. Therefore a high correlation with an observed temperature time series would not necessarily demonstrate any model skill.

In Figure 2 the three ensemble members are represented by the dashed lines. The correlation with the observed temperatures is very high even though data points over ocean have been excluded. The dashed lines show a fairly small spread which represents a small model uncertainty. Nevertheless the solid grey line is right in between the dashed lines for many time intervalls.

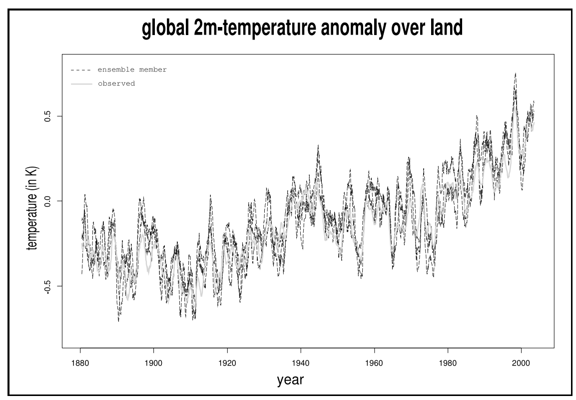

Figure 2: simulated ECHAM 5 temperature anomalies for $20th$ century

From the atmospheric simulations the global axial AAM is calculated by the integration shown in Equation 7. The model is discretising zonal windspeed on 31 model levels (η-levels). To avoid interpolation through mountains the vertical integration is done over these hybrid η-levels. In contrast to pressure levels these levels follow the terrain and they are by definition above surface. That's why integrations over pressure levels tend to overestimations in global axial AAM.

Observed ΔLOD variations (C04 series of the IERS) are plotted together with the simulated

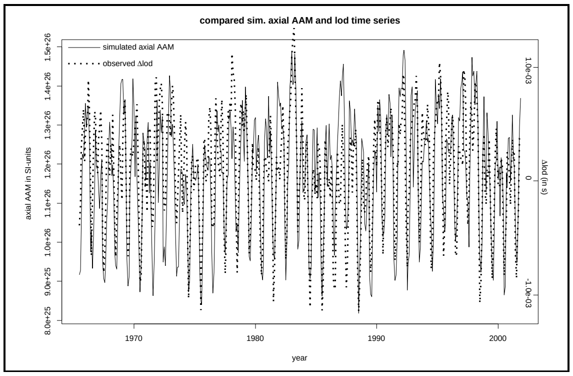

Figure 3: time series of simulated axial AAM and ΔLOD (7yr running mean removed)

AAM time series. Decadal changes due to core-mantle-interaction have been removed from the observations by a seven year running mean. The effect of long-periodic tides has been removed by filtering. Short periodic tide effects are purged by only considering monthly mean values. The remaining signal is highly correlated with the axial relative AAM time series. Not only the annual and semi-annual cycle but although the El Niño peaks are well reconstructed. A fingerprint of these typical oscillations can be found in the wavelet spectrum of the sim. AAM (Fig. 4). A lot of energy remains in a broad band with periods from three to six years. These oscillations are excited by ENSO.

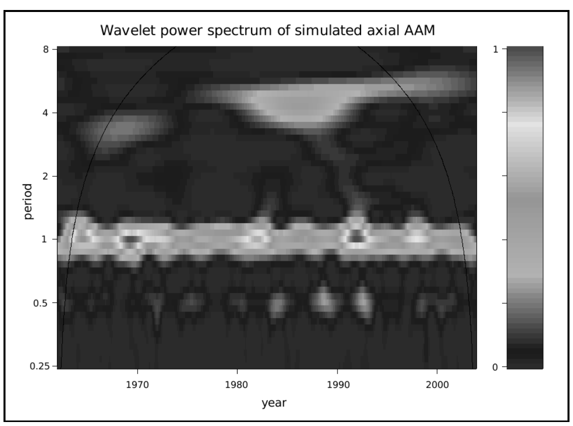

Figure 4: wavelet power spectrum of sim. axial AAM (period 1962 to 2003)

The scenario runs show a strong trend in the axial AAM (Fig. 5). Under this A1B climate change scenario the atmosphere induces an increased global AAM. The increase quantifies 10 percent for the year 2100 according to the 2001 to 2010 reference period.

In Figure 6 trends of zonal windspeeds at 300 hPa are displayed. In the southern hemisphere the antarctic circumpolar current gets boosted. Generally trends over land are weaker. All in all the change pattern is in good consistency with the results of former studies (Lorenz and DeWeaver, 2007).

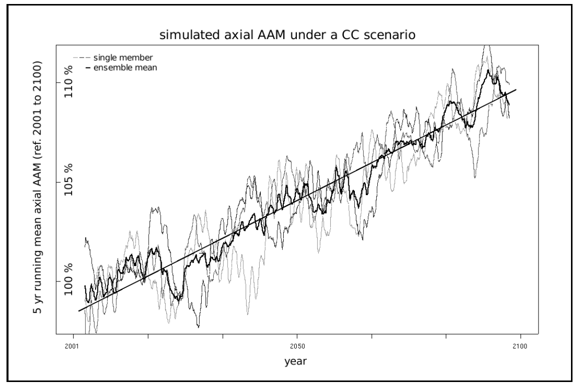

Figure 5: time series of ECHO-G A1B scenario of global axial AAM (5 yr running mean)

For the year 2100 the increased axial AAM in the model would lengthen the day by about $0.65ms$. Integrating over the whole 21_{st} century results in a delay of about 11.86s. One has to keep in mind that other effects were not considered, so this is only due to the motion term of the atmosphere. For instance the AM loss to the moon will lead to an Earth's rotation which is 40s behind schedule for the year 2100.

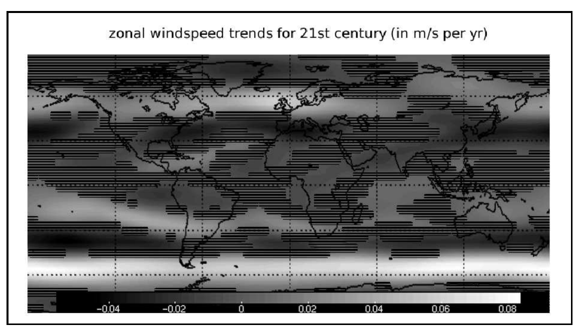

Figure 6: zonal windspeed trends at 300hPa for 21_{st} century of ensemble mean (shaded areas have no significant trend)

5 Discussions

All in all the ECHAM 5 simulations of atmospheric effects on LOD are very promising. The well reproduced global temperature anomaly time series is hinting at realistically reconstructed circulation patterns. Concerning simulated axial AAM not only characteristics in frequency space but although amplitudes are very well captured and exceed results of previous low resolution GCM studies in quality. Possible improvements should be achieved at the boundaries of the troposphere. Winds within the boundary layer are highly influenced by an unrealistic orography and simulated winds at the tropopause may have big absolute errors due to big magnitudes and due to a rudimentary illustration of the stratosphere within the model. Obviously higher model resolution tends to produce more realistic results, which is not trivial as we are dealing with axial AAM - a globally integrated variable (Stuck, 2002).

ECHO-G A1B scenario runs show a very strong centurial increase in AAM. The dynamic reason of the increase cannot be retraced easily. Strongly increased temperatures in the upper tropical troposhere enhance the meridional temperature gradient. In the inner tropics the tropopause level is rising therefore the tropopause slope towards the poles is getting intensified. Stratospheric cooling and tropospheric warming amplify the meridional temperature gradient. Due to thermal wind balance westerlies become stronger. The increase in kinetic energy at the tropopause level is consistent with the rise in tropopause height because synoptic waves are trapped in the troposphere (Lorenz and DeWeaver, 2007). For validation purpose one should compare results to other state-of-the-art models. The amplitude of zonal windspeed trends seems a bit overestimated (de Viron, 2002). Generally the ECHO-G model was not an outlier in terms of IPCC temperature projections.

6 Acknowledgements

This paper was developed within a project supported by DFG grants HE 1916/9-1 and DR 143/12. The authors thank the Deutsches Klimarechenzentrum (DKRZ), Hamburg, Germany, for providing the CPU time for the standalone runs and Seung-Ki Min for providing the ECHO-G data sets.

7 References

de Viron, Geophysical Research Letters, VOL. 29, NO. 7, 10.1029/2001GL013672, 2002.

Fröhlich, C. and Lean, J.: The Sun's total irradiance: Cycles, trends, and related climate change uncertainties since 1976, Geophysical Research Letters 25(23), 4377, 1998.

Gross, R. S., I. Fukumori, D. Menemenlis, and P. Gegout: Atmospheric and oceanic excitation of length-of-day variations during 1980-2000. J. Geophys. Res., 109, B01406, doi:10.1029/2003JB002432, 2004.

Hide, R., Nature 222, 1055 - 1056; doi:10.1038/2221055a0, 1969.

Lambeck, K.: The Earth's Variable Rotation: Geophysical Causes and Consequences. Cambridge University Press, New York, 1980.

Lorenz and DeWeaver, J. Climate, 16, 132-143, 2007.

Roeckner, E. et al.: The atmospheric general circulation model ECHAM 5. PART I: Model description, Rep. 349, MPI for Meteorology, Hamburg, Germany, 2003.

Rosen, R. D., and W. J. Gutowski: Response of zonal winds and atmospheric angular momentum to a doubling of CO2. J. Climate, 5, 1391-1404, 1992.

Stuck, J.: Die simulierte axiale atmosphärische Drehimpulsbilanz des ECHAM3-T21 GCM, PhD thesis, Bonner Meteorologische Abhandlungen, 56, Asgard, Sankt Augustin, 2002.

Taylor, K.E., D. Williamson and F. Zwiers: The sea surface temperature and sea-ice concentration boundary conditions of AMIP II simulations. PCMDI report No. 60, 20 pp, 2000.